STØTTET AF
Promilleafgiftsfonden for landbrug
Ministeriet for Fødevarer, Landbrug og Fiskeri
gudp

Agricultural and Forest Meteorology 344 (2024) 109790

Contents lists available at ScienceDirect

Agricultural and Forest Meteorology

journal homepage: www.elsevier.com/locate/agrformet

Experimental and model-based comparison of wind tunnel and inverse dispersion model measurement of ammonia emission from field-applied animal slurry

Sasha D. Hafner, Jesper N. Kamp, Johanna Pedersen *

Department of Biological and Chemical Engineering, Aarhus University, Blichers Alle 20, Tjele 8830, Denmark

ARTICLE INFO

Keywords:
NH_3
Micrometeorology
Emission dynamics
Emission factor
Mass transfer model
Backward Lagrangian stochastic model

ABSTRACT

Volatilization of ammonia from field-applied animal slurry is a significant problem. Accurate emission measurements are needed for inventories and research, but are not provided by all measurement methods. Wind tunnels may give emission values substantially above or below micrometeorological results, which have been shown to be accurate. This limitation reduces the utility of wind tunnel results, which make up a large fraction of available measurements. The present work focused on understanding wind tunnel measurement error by comparing micrometeorological and wind tunnel measurements with the aid of a semi-empirical model. Ammonia loss from digestate after field application was measured in high time resolution in three field trials using wind tunnels and the backward Lagrangian stochastic (bLS) dispersion technique simultaneously. Differences in measured emission were interpreted using the ALFAM2 model, and measurements were used to evaluate the model. Results showed that wind tunnel and bLS methods provided different cumulative emission estimates, although there were similarities in measured emission dynamics. The ALFAM2 model was generally able to reproduce emission dynamics for both measurement methods, but only when differences in mass transfer between the two methods were incorporated in an experimental parameter set. This important result suggests that: 1) the simple structure of the ALFAM2 model captures the essential physical and chemical processes controlling emission and 2) the two measurement methods differ only (or mainly) through mass transfer above the slurry/soil surface and rain. Therefore, with careful selection of wind tunnel air flow it should be possible to approximately match emission that occurs under open-air conditions. But without temporal variation in air flow, actual emission dynamics cannot be captured. This work provides a template for integrating and comparing measurements from different methods, and suggests it is possible to use wind tunnel measurements for model evaluation and even parameter estimation.

1. Introduction

The agricultural sector is a significant source of emissions, including ammonia (NH_3), greenhouse gases, and volatile organic compounds, all of which have negative effects on the environment and human health (Houlton et al., 2019). Emission occurs throughout the livestock production chain, with livestock housing, manure handling and storage, and field application all contributing (Uwizeye et al., 2020). Field application of liquid manure (slurry) will always pose a risk of environmental pollution due to volatilization of NH_3. Research on this topic over the past few decades has resulted in an increased knowledge on specific parameters affecting NH_3 emission dynamics (e.g., Sommer et al., 2003, 2006; Pedersen, Nyord, et al., 2021), models that can be used to predict emission (e.g., Génermont and Cellier, 1997; Huijsmans et al., 2018; Hafner et al., 2019), and development of different low-emission application techniques (e.g., Nyord et al., 2008; Webb et al., 2010; McCollough et al., 2022) and slurry treatments (Fangueiro et al., 2015; Pedersen et al., 2022). Some of these results have been put into practice; several countries have policies or regulations aimed at reducing NH_3 emission after field application of slurry (Aneja et al., 2009; Huijsmans et al., 2016). Despite this progress, the complex processes involved in NH_3 emission are not completely understood, making accurate prediction of observed variation in ammonia loss challenging (Hafner et al., 2019).

* Corresponding author.
E-mail address: jp@bce.au.dk (J. Pedersen).

https://doi.org/10.1016/j.agrformet.2023.109790
Received 22 December 2022; Received in revised form 23 October 2023; Accepted 27 October 2023
Available online 10 November 2023
0168-1923/© 2023 The Author(s). Published by Elsevier B.V. This is an open access article under the CC BY license (http://creativecommons.org/licenses/by/4.0/).

Several different methods can be used to measure NH_3 emission after field application of slurry. They can roughly be sorted into two categories: micrometeorological methods and enclosure methods. Micrometeorological methods include integrated horizontal flux (IHF) and the backward Lagrangian stochastic (bLS) dispersion technique. Enclosure methods include wind tunnels which is a type of enclosure method with continuous (primarily longitudinal) airflow (Shah et al., 2006). Micrometeorological methods do not affect emission because they do not manipulate airflow or atmospheric conditions above the emitting surface. The resulting flux measurements are considered accurate based on results from gas release experiments (Flesch et al., 2004; McBain and Desjardins, 2005; Yang et al., 2016). Furthermore, slurry can be applied by full-scale farm machinery, which can be a challenge with enclosure methods.

Adsorption of NH_3 in the sampling system and analyzers and deposition between the source area and the sensor can cause biases in emission estimation. These challenges make it difficult to measure NH_3 emission using eddy covariance (EC) with a closed path analyzer, because EC requires high-frequency measurements and adsorption will dampen the response. Simultaneous release of NH_3 and methane gas with an open path analyzer and a line integrated system showed approximately 10 % lower recovery for a closed path system with bLS (Lemes et al., 2023). Heating and increased sampling line flow are the key to minimize loss of NH_3 in the sampling system. However, continuous measurements at a single location should not lead to loss of NH_3, but rather a dampening of temporal variability or memory effect by longer response time.

Micrometeorological methods can be challenging to implement because wind profiles should be undisturbed in order to meet the assumptions implicit in emission calculations. Therefore, large homogeneous field plots without large objects (buildings, trees, etc.) are required (Businger, 1985; Loubet et al., 2010), making replication challenging. On the other hand, the large scale of micrometeorological field trials can reflect normal random variation in e.g., soil properties and uneven application with full-scale machinery. Replication is much easier with wind tunnels, which only require a small plot area. Unlike micrometeorological methods, wind tunnels do not rely on natural air movement and therefore avoid periods where calculation assumptions are not valid leading to less data loss. But wind tunnels change the airflow over the emitting surface, prevent precipitation, and affect surface heating (Scotto di Perta et al., 2020). The slurry is often applied manually in wind tunnel experiments to avoid application outside the wind tunnel plot area, ensuring that air entering the tunnel has low concentrations of NH_3 and emission is not suppressed (Wulf et al., 2002; Misselbrook et al., 2005; Bell et al., 2015).

Wind tunnel design affects emission as the air movement inside the tunnel determines mass transfer, with higher air exchange rates (AER) resulting in higher NH_3 flux (Eklund, 1992; Smith and Watts, 1994; Sommer and Misselbrook, 2016). The longitudinal air velocity or speed (m s^{-1}) is commonly reported in studies using wind tunnels. This value is sometimes measured as a speed within the emission chamber and other times calculated as an average velocity based on the volumetric flow rate and the cross-sectional area of the emission chamber. Neither the measured nor calculated average values provide insight into the variations of air velocity that are known to occur within the chamber (Jiang et al., 1995; Loubet et al., 1999; Scotto di Perta et al., 2016) or the mass transfer coefficient near the soil surface, which depends on the velocity profile and turbulence intensity (Loubet, Cellier, Génermont, Flura, 1999). Flux has been found to increase with air velocity and turbulence intensity (Sommer et al., 1991; Mannheim et al., 1995), and decrease with wind tunnel size, probably due to differences in velocity profiles and turbulence (Saha et al., 2011).

Other studies have compared micrometeorological measurements with wind tunnel measurements after field application of slurry. Some found a good correlation in trials or periods without precipitation and moderate to high wind speed as long as the air velocity or speed within the emission chambers was controlled to be equal to ambient wind (Ryden and Lockyer, 1985; Mannheim et al., 1995), whereas other trials or measuring periods showed under- or overestimation by the wind tunnels (Ryden and Lockyer, 1985; Mannheim et al., 1995; Misselbrook et al., 2005; Scotto di Perta et al., 2019). These studies all used relatively low temporal resolution to compare methods, with a measurement frequency of 4 – 11 d^{-1}. Systems with high-frequency measurements in the field can provide shorter measurement intervals, for example a frequency of 14 d^{-1} for wind tunnels (Pedersen et al., 2020) or 48 d^{-1} for bLS (Kamp et al., 2021). This level of detail could provide more measurements for comparison in a single trial, but also facilitates comparison of emission dynamics, which may be more useful than cumulative emission for understanding differences.

As new slurry application methods and slurry treatments are developed with the purpose of mitigating NH_3 emission (Fangueiro et al., 2017; McCollough et al., 2022), it is necessary to be able to evaluate and compare them with a reference scenario so end users and policy makers have sufficient knowledge for decision making. Methods that allow replication and simultaneous evaluation of multiple treatments, such as wind tunnels, are therefore useful. Even though these features are difficult to implement in micrometeorological methods, the estimates of absolute emissions they provide are essential. Careful consideration about the objectives of the research is necessary before selecting which method to use.

Measurement of NH_3 loss from field-applied slurry is labor-intensive and expensive, and generally only one or two of the parameters influencing emission can be studied at the same time. Varying climatic conditions, changes in soil and slurry properties, and different measuring methods between experiments complicate direct comparisons of results, making it difficult to draw general conclusions (Hafner et al., 2018). modeling can be used to overcome some of these challenges, and models are often used to estimate emission factors for national inventory reporting and legislative purposes. The ALFAM2 model (Hafner et al., 2019) is a flexible semi-empirical dynamic model for predicting NH_3 emission from field applied slurry that has been used for research (Pedersen et al., 2022; Andersson et al., 2023) and inventory calculations (Hafner et al., 2021).

Empirical models require measurement data for parameter estimation, and even mechanistic models require measurement data for evaluation. The numeric values of ALFAM2 model parameters (see Section 2.4 for more details), which describe effects of application method, slurry properties, and weather on emission, have been determined from fitting to measurements available in the large public ALFAM2 database (Hafner et al., 2018, Hafner, Adani, et al., 2023). Because of the challenge in determining absolute emission from wind tunnel measurements, so far only micrometeorological measurements have been used for estimating parameter values for the ALFAM2 model (Hafner et al., 2019, 2021). A large number of wind tunnel observations, which undoubtedly contain useful information about NH_3 emission, have been excluded (nearly 700 of 2200 plots in the database). A better understanding of differences between wind tunnel and micrometeorological measurements could facilitate the use of these measurements.

Two questions are relevant to the problem of using wind tunnel measurements for parameter estimation, and more generally, in understanding the value of wind tunnel results compared to micrometeorological methods. First, are wind tunnel results representative of plausible weather conditions? Stated differently, do wind tunnel measurements reflect natural emission that could be expected to occur? If so, is it reasonable to rely on differences in emission between e.g., application methods or slurry properties measured using wind tunnels? Second, how can wind tunnel and micrometeorological measurements be quantitatively related? Without some approach accounting for emission biases resulting from wind tunnel use, it is difficult to use wind tunnel results for direct estimation of emission factors or model parameters. It is difficult to answer these questions through a direct comparison of flux or cumulative emission measured with the two methods, because NH_3 flux measured at any particular time depends on the cumulative history of mass transfer to the atmosphere and into the soil up to that point. In this work, we applied the ALFAM2 model to address this challenge. The model was applied to high-resolution online NH_3 emission measured simultaneously after field-applied slurry with bLS and wind tunnels in three field trials. In addition, the default parameter set for the model was itself evaluated using the bLS measurements. Digested slurry was chosen as the slurry type for the trials because an increasing amount of slurry is digested or co-digested for biogas production prior to field application (Abanades et al., 2022). Studies measuring emission after field application of digested slurry are rare, resulting in a higher uncertainty in emission factors (Hafner et al., 2021).

2. Materials and methods

2.1. Overview of field trials

Three field trials were conducted, each including NH_3 emission measured simultaneously in different plots on the same field (size of the field: 3.5 ha) with the bLS method and wind tunnels (see Fig. 1 for field trial layouts). The trials were conducted over one week in three different periods at the same field (Aarhus University, Campus Viborg; 56.493412, 9.561302) with the same slurry. Two trials were conducted in August 2021 (2021–08–11 and 2021–08–20) and one trial in January 2022 (2022–01–05) as different climatic conditions were desired. The emissions were measured for 168 h in each field trial.

Calculations and data can be found in a GitHub repository (https://github.com/AU-BCE-EE/Hafner-2022-bls-wt-comp) and the version presented here is archived as a Zenodo dataset (Hafner, Pedersen, Kamp, 2023).

2.2. Slurry and soil properties, slurry application, and climatic conditions during the trials

Before the first trial, approximately 30 tonnes of digested slurry (digestate) was pumped from a storage tank to a concrete storage tank covered with a concrete lid to be used for all three trials. The digestate was produced at the biogas plant at Aarhus University, which operates two reactors in series. Reactor 1 was operated at 51 °C and had a retention time of 14 days, whereas reactor 2 was operated at 47 °C with a retention time of 40 days. After the second reactor, the digestate was pumped to the concrete storage tank where the digestate for the trials in the present study was collected. The input to the first reactor in the period where the digestate was produced for the trials was 70 % cattle slurry (by fresh mass), 14 % silage (primarily grass), 9 % grass, 7 % pig slurry, and small amounts of poultry feed and horse manure.

For the measurements with the wind tunnels, the slurry was applied manually with a watering can with a hose attached to mimic trailing hose application For the bLS measurement, the plots were 588, 778, and 335 m^2 for the first and second trial in August and the third trial in January, respectively. Slurry was applied with trailing hoses by a 16-m wide slurry boom with 30 cm between the hoses (hose diameter: 45 mm). The tractor had a driving speed of approximately 7–8 km h^{-1}. The application rate of the machinery used to apply digestate in the bLS plots was determined by weighing the tractor and slurry tank before and after an application. For both wind tunnels and bLS measurements, 35.9 tonnes ha^{-1} was applied in the three trials.

The soil was a loamy sand and barley had been sown in the previous spring. Harvest occurred prior to the trials, so stubble (about 5 cm) was present during all three. The soil had a 1:1 water pH of 5.4 ± 0.2 (± standard deviation, $n = 3$). Dry bulk density and gravimetric water content were determined using 100 cm^3 soil cores taken at 0–5 cm depth. The dry bulk density was 1.29 ± 0.17 ($n = 9$) and the gravimetric water content was 0.21 ± 0.004, 0.21 ± 0.01, and 0.27 ± 0.03 g^{-1} ($n = 3$) at the beginning of the first and second trial in August and the third trial in January, respectively.

Slurry DM content was determined by drying at 105 °C for 24 h (American Public Health Association, 1999), total nitrogen was determined with the Kjeldahl method by distillation and titration (Association of Official Analytical Chemists, 1999), and total ammoniacal nitrogen (TAN) was determined photometrically (International Standard, 1984). All analysis and application rates during the trials can be found in Table 1.

The surface pH of the slurry after application was measured in the field with a flat surface pH electrode (Orion™ 8135BN ROSS™, Combination Flat Surface pH Electrode, Fischer Scientific, Loughborough, UK). The method vas validated previously (Pedersen, Andersson, et al., 2021). The electrode was placed in the slurry band as close to the slurry-air interface as possible. Two additional slurry bands only for measuring the pH were made close to the wind tunnel system. One was covered with a plastic sheet to protect the slurry from precipitation but allow airflow over the slurry surface to mimic conditions inside the wind tunnels. The other was left unprotected to have the same conditions as the bLS plot. The plastic sheet might have affected the emissions, and thereby the pH, of the slurry band covered. The covering might reduce emissions by reducing the air transfer over the slurry surface, whereas it might increase emission in experiments where precipitation occurred.

2.3. Emission measurements

All concentration measurements were performed with cavity ring-down spectrometer (CRDS) instruments (G2103 NH_3 concentration Analyzer, Picarro, CA, USA). Two instruments were used for the bLS measurements (one for background and one for plot concentration) and one instrument was used for the wind tunnel measurements. These instruments have been shown to be robust and reliable in agricultural environments (Kamp et al., 2019).

2.3.1. Wind tunnels

Nine wind tunnels were used to continuously measure NH_3 emission with a CRDS. The wind tunnel system was described in detail by Pedersen et al. (2020), including an evaluation of mass transfer by comparing evaporation of ethanol inside the emission chamber at different positions with evaporation outside the chambers. The system is summarized here, and a sketch of the tunnels can be found in the

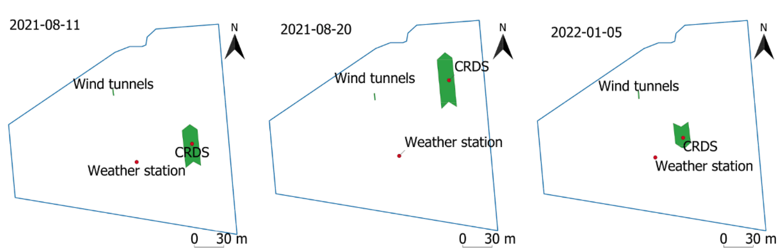

Fig. 1. Field layout for the three field trials. Placement of wind tunnels, weather station (including background measurement position for bLS), and CRDS analyzer measuring NH_3 concentration for bLS. Blue line shows field edges and green areas show where slurry was applied.

Table 1
Digested slurry properties (± standard deviation, $n = 2$) and application details.

Application time	Application rate (kg TAN ha^{-1})	DM (%)	Total N (g kg^{-1})	TAN (g kg^{-1})	pH	
					Field[a]	Laboratory[b]
2021–08–11 16:15	68	5.31 ± 0.03	2.80 ± 0.04	1.90 ± 0.10	7.7	7.7 ± 0.1
2021–08–20 10:51	70	4.95 ± 0.08	2.80 ± 0.04	1.95 ± 0.10	7.9	7.6 ± 0.1
2022–01–05 13:26	62	4.47 ± 0.06	2.49 ± 0.13	1.72 ± 0.03	7.9	7.8 ± 0.1

[a] Measured in the field immediately prior to application.
[b] Measured in the laboratory after storing for 1 day at 5 °C.

supplementary material (Fig. S1). Each wind tunnel consisted of an open-bottomed stainless-steel chamber (25 cm height, 80 cm length and 40 cm width). A motor with a fan was connected to the downwind end of the chamber via a steel duct to control the emission chamber airflow, which was held constant for each tunnel during each trial. The air inlet was a narrow slot only 1.3 cm high to increase resistance of the air flow through the chamber and thereby stabilization of the fans. Furthermore, the small air inlet prevents back-flow, which might lead to false high measurements of the background concentration. During each of the trials three tunnels had a volumetric air exchange rate (AER) of 25 min^{-1} (m^3 flow per minute per m^3 chamber volume) (average air velocity of 0.33 m s^{-1}, see Section 2.4 for more information). In the first August trial, two tunnels were operated with an AER of 20 min^{-1} and two with an AER of 30 min^{-1}. During the second August trial and the January trial, two and three tunnels, respectively, were operated with an AER of 7 min^{-1} and 54 min^{-1}. Each tunnel was mounted on a metal frame (inner length: 67.4 cm, inner width: 29.3 cm) which was inserted into the soil, giving a field plot area of 0.2 m^2. A subsample of air was drawn from the tunnels at 1.4 L min^{-1} through heated PTFE tube (OD: 6.35 mm, ID: 4.75 mm) to a 10 or 19 port rotary valve (VICI, Valco Instruments Co. Inc., Houston, TX, USA). The air was sampled from the duct between the emission chamber and the fan through a y-shaped inlet with quadratically spaced sampling points (configuration C3u (ii) in Loubet, Cellier, Flura, Génermont, 1999). Three open-ended tubes for measuring the NH_3 concentration in the air entering the chambers (background air) were evenly distributed between the tunnels. The length of the tubes for sample and background air ranged from 5 to 10 m. Each measurement required 8 min, yielding a data point every 80 min for each sampling point (tunnel and background) during the two trials in August (seven tunnels and three backgrounds) and every 104 min during the trial in January (nine tunnels, three backgrounds and one background 20 m away from the setup). Only the background measurements from the air entering the tunnels were used for calculations.

The recovery of NH_3 was tested throughout the system prior to each trial by adding a standard gas (98.9 ± 3.0 ppm NH_3) to the inlet of one of the tubes. The recovery was found to be minimum 95 % within the 8-minute measurement interval.

An average of the last 30 s of measurements per 8-minute measurement cycle was used for calculations of the flux and cumulative emission. An average of the background measurements ($n = 3$ locations) was subtracted for each measurement cycle concentration before further calculations. The flux, (F, mg s^{-1} m^{-2}), was calculated from the background-corrected concentration (C, mg m^{-3}), the air flow in the emission chamber (q, m^3 s^{-1}), and the area of the soil surface covered by the tunnel (A, m^2) (Eq. (1)).

$$F = \frac{C \cdot q}{A} \tag{1}$$

The beginning of an 8-minute measurement cycle was taken as the start of each 80 or 104 min measurement interval, and average flux and interval emission was calculated for each interval using the trapezoidal integration rule (Simmons, 1996). Measurement data were submitted to the ALFAM2 database and are available as plot-measurement method keys (pmid) 1904 through 1925 (v2.22, Hafner, Adani, et al., 2023).

2.3.2. The backward Lagrangian stochastic model

The bLS model (Flesch et al., 2005) embedded in the software R in form of the bLSmodelR package (https://github.com/ChHaeni/bLSmodelR, v4.3, Häni et al., 2018) was used to estimate the emission rate of NH_3 in half-hourly intervals. The model estimates a concentration-to-emission ratio (CE_{bLS}) for each interval by calculating upwind dispersion from the position of the concentration sensor. The ratio is then used to calculate flux (Eq. (2)).

$$F = \frac{C_{downwind} - C_{upwind}}{CE_{bLS}} \tag{2}$$

In Eq. (2), F is the NH_3 flux (mg s^{-1} m^{-2}) and $C_{downwind}$ and C_{upwind} are NH_3 concentrations (mg m^{-3}) measured down- and upwind of the slurry covered area, respectively. These calculations are backward in time and the number of backward trajectories calculated can be increased to improve the model estimate. In these trials, 1 million trajectories were calculated for each interval using a computer cluster. The trajectories touching the ground inside the source area and the vertical touchdown velocities were used to calculate CE_{bLS} (see Häni et al., 2018 for further explanation).

The bLS model relies on accurate measurements of wind statistics, up- and downwind concentrations, and relative position between sources and sensors. The wind statistics were measured at 16 Hz with an 3D ultrasonic anemometer at 2 m (WindMaster, Gill Instruments Limited, Lymington, UK).The Monin-Obukhov Similarity Theory (MOST) was applied to get estimates of friction velocity (u^*), stability defined by the Monin–Obukhov length (L), the roughness length (z_0), the standard deviation of the wind components normalized by the friction velocity (σ_u, σ_v, σ_w), and the wind direction. The concentration of NH_3 was measured 0.5 m above the surface with two CRDS instruments. The PTFE inlet tubes for the CRDS analyzers were insulated with hot wires between the tube and the insulation and heated to approximately 40 °C. The sampling positions and the outline of the plot area were mapped out with a pole-mounted GPS receiver (Trimble R10, Sunnyvale, California, USA). Concentration measurements are most often conducted some distance away from the source depending on the source height, but here the source was a flat field, which allows for concentration measurements inside the source area. This means the plume from the source was caught at all wind directions leading to less data exclusion. This approach has been tested and verified against measurements outside the source area after field application of slurry (Kamp et al., 2021).

Within an averaging interval, the conditions were assumed to be stationary, and the source was assumed to have a spatially homogeneous emission strength. Evaluations of the bLS model have shown error of 10 % or less from experiments with release of known quantities of a target gas (Flesch et al., 2004; McBain and Desjardins, 2005; Harper et al., 2010; Yang et al., 2016; Lemes et al., 2023). The uncertainty in a single interval can be larger. Performance of the bLS model is dependent on the atmospheric conditions, thus filtering of the data is a necessity for high accuracy (Flesch et al., 2004). Data were removed when either $u^* < 0.05$ m s^{-1}, $|L| < 2$ m, $z_0 > 0.1$ m, $\sigma_u / u^* > 4.5$, $\sigma_v / u^* > 4.5$, or $C_0 > 10$ (Bühler et al., 2021). C_0 is the Kolmogorov constant of the Lagrangian structure function. The filtering removed 19 % to 33 % of the measurement intervals from the three trials. To properly estimate the overall cumulative loss of NH_3 during the measurement without underestimation due to the removal of the filtered data, gap filling was necessary. Gap filling will introduce uncertainty in the cumulative TAN loss, but the alternative is a certain underestimation. Gap filling was done by linear interpolation between valid points, with most of the gap filling during night when the lowest emission was observed. The cumulative loss of NH_3 with filtered data removed was 17 % to 26 % lower than when gap filling was applied to the removed periods. Measurement data were submitted to the ALFAM2 database and are available under plot-measurement method keys ("pmid") 1935, 1936, and 1938 (v2.22, Hafner, Adani, et al., 2023).

2.4. ALFAM2 model application

The ALFAM2 model was applied for two purposes in this work: 1) to aid in the interpretation of differences between wind tunnel and bLS measurements of emission, and 2) to evaluate the model structure and the current default parameter set (set 2) with emission measurements (Section 2.3). The ALFAM2 R package (v3.5, https://github.com/sashahafner/ALFAM2) (Hafner et al., 2022) was used in the R environment (v4.2.1) (R Core Team, 2022) to make all model calculations. A brief description of the model and software package is given here; for more details see Hafner et al. (2019).

Immediately following slurry application, the ALFAM2 model partitions TAN between "slow" and "fast" pools, where the slurry in the fast pool is in close contact with the atmosphere and the slow pool represents slurry with a lower emission rate due to soil infiltration or other processes. Mass of TAN is then tracked over time, using a closed-form solution to a set of differential equations that can be applied to any time step size (interval duration) without a loss of computational accuracy, typically matching the temporal resolution (measurement frequency) of weather inputs. Applied TAN may only volatilize or remain in one of the two pools; the model does not include any conversion processes. The model has five "primary" parameters that describe rates of NH_3 loss or transfer between pools, and their values are linked to a set of predictor variables, such as weather conditions, slurry dry matter (DM), and application technique (Fig. 2). This structure (Fig. 2) is a simplified representation of the physical-chemical slurry-soil-atmosphere system, with multiple complex processes (e.g., chemical speciation, diffusion, advection) lumped into parameters with empirical values. The software package includes a default parameter set, currently "set 2" (Table S1). As described elsewhere, these parameter values were determined from fitting to micrometeorological emission measurements from the ALFAM2 database (Hafner et al., 2018, 2021). Inclusion of particular predictor variables depends on availability of sufficient measurements for parameter estimation. For example, no soil properties are included as predictor variables.

The first purpose of ALFAM2 model application (interpretation of differences between wind tunnel and bLS measurements) was realized by application of the model to both measurement methods together. A

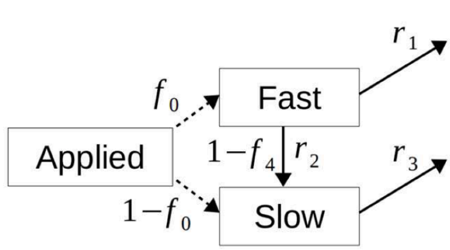

Fig. 2. The structure of the ALFAM2 model (based on Hafner et al., 2019). Applied TAN is immediately partitioned between two pools upon slurry application. Five primary parameters together determine partitioning, transfer between pools, and emission. Model parameters control instantaneous TAN partitioning (f parameters, f_0 for initial and f_4 for incorporation) or mass transfer rate (first-order r parameters) and their values are related to various predictor variables.

new "experimental" parameter set developed for this task (referred to as "set E" for experimental) included different values for bLS and wind tunnel for those parameters related only to mass transfer. Parameter set E included: intercept terms for f_0 and r_2, separate intercept (constant) terms for bLS and wind tunnel for r_1 and r_3, air temperature parameter for r_1, separate parameters for wind tunnel air velocity and bLS wind speed effects on r_1 and r_3, and a rainfall parameter that affects r_2 (Fig. 2). Together these particular parameters reflect a conceptual model where differences between these two measurement methods are related only to mass transfer of TAN in the two pools to the atmosphere and a lack of rainfall. Differences in mass transfer are captured in the different intercept and air velocity or wind speed terms for r_1 and r_3. Ammonia that volatilizes from field-applied slurry undergoes mass transfer both within slurry (or soil) and air above the surface (Génermont and Cellier, 1997; Sommer et al., 2003) but these processes are lumped together in the ALFAM2 model. Here we hypothesize that r_1 and r_3 differences between the two measurement methods are due only to differences in mass transfer within air above the slurry/soil surface, i.e., air-side mass transfer. Parameter estimation was based on minimizing the difference between measured and calculated interval flux F. The optim() function from the stats package in base R (v4.2.1) (R Core Team, 2022) was used with the gradient-based quasi-Newton method of Byrd et al. (1995) (method = "L-BFGS-B"). A nonparametric bootstrap approach was used (Davison and Hinkley, 1997) to estimate approximate standard error for parameter estimates. In the bootstrap approach three bLS and 22 wind tunnel plots were randomly selected with replacement in each of 100 iterations (i.e., resampling with replacement), matching the total number of each type of measurement technique in the complete dataset in each iteration. Lack of stratification among dates or wind tunnel AER and the small number of bLS plots limit the accuracy of these standard error estimates, but the method provides an estimate of precision.

The two purposes of ALFAM2 model application are not completely distinct. Whether or not the model can be applied simultaneously to both wind tunnel and bLS measurements, and the structure and numeric values of parameter set E, has implications for both interpreting wind tunnel measurements and the accuracy of the model. The second purpose (evaluation of the model) therefore also relied on the performance of parameter set E. But the default parameter set 2 was also evaluated by comparison between model predictions and measured emission. The ALFAM2 model was applied to both bLS and wind tunnel measurements. Considering the model structure (Fig. 2), there is no fundamental reason it would apply to one method and not the other, but the default parameter values were based on (and are intended to represent) micrometeorological measurements. Application of the model to bLS measurements was straightforward; measured air temperature and average air speed (measured at 2 m height) within each interval were used along with manure properties and application details to predict NH_3 loss over time. For wind tunnel measurements, calculated average air velocity within the wind tunnel was used as a surrogate for average natural wind speed. This substitution is known to be problematic, as discussed in detail previously (Andersson et al., 2023). The relationship between mass transfer and average air velocity within a wind tunnel depends on wind tunnel design, and earlier measurements made with this particular design suggest that the wind tunnels provide similar mass transfer rates at much lower numeric values of average air velocity, compared to natural wind speed (Pedersen et al., 2020). Average velocity and AER are related through the ratio of chamber volume to cross-sectional area, which was the chamber length (0.8 m).

3. Results and discussion

3.1. Ammonia loss and effects of weather

The weather was similar for the two trials in August; air temperature ranged from around 10 to 22 °C with a mean value of 15 °C and wind speed at 2 m above ground ranged from below 0.2 to above 5 m s^{-1}, with a mean of 2.3–2.4 m s^{-1} (Fig. 3). Air temperature was much lower in the January trial: −3.4 to 9 °C with a mean of 2.5 °C, and wind speed was only slightly higher with a mean of 2.8 m s^{-1} (Fig. 3). Regular diurnal patterns were obvious in temperature with peaks a few hours after midday (around 15:00). Wind varied as well with the lowest wind speeds at night, but less regularly. Precipitation was very low over the first two days in all three trials (maximum of 1.5 mm over first 48 h in January). Total precipitation was 0.6 mm for the second August trial and higher for the other two. Ammonia flux peaked at or near the start of measurements, rapidly declined over the first ½ day, and remained at a much lower level for the duration of the trials (Fig. 3). This pattern is typical for NH_3 loss from field-applied slurry (Hafner et al., 2018). Peak flux in the January trial was lower for all plots than during the two warmer August trials (Fig. 3). There was some indication of peaks in NH_3 flux at later times associated with high air temperature or wind speed. With only low precipitation over the first two days, large effects on NH_3 emission were unlikely.

Cumulative emission varied widely among the trials and measurement methods, from 17 % to 55 % of applied TAN (Fig. 4). As expected, NH_3 loss was the lowest for the coldest third trial. Despite similar

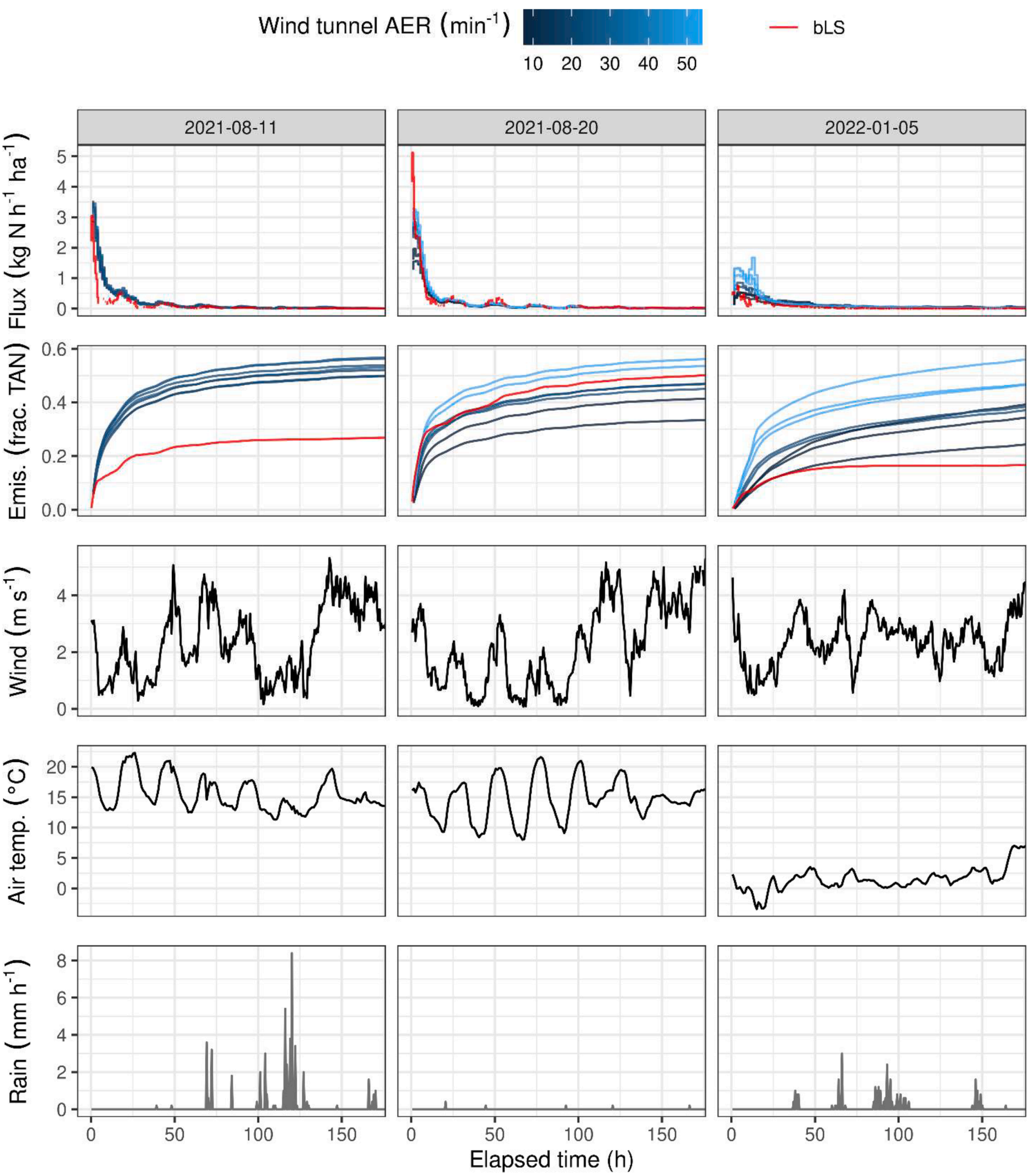

Fig. 3. Field trial results showing measured ammonia flux and cumulative emission (as a fraction of applied TAN) calculated from the flux (top two rows) along with weather conditions measured at the field site (30 min averages). Wind speed was measured at 2 m height. Red lines show bLS measurements, and blue wind tunnel, while the intensity of blue represents the magnitude of the air exchange rate within wind tunnels (see legend). Interpolated values are omitted from the flux lines for bLS but are included in the cumulative emission curves. AER: volumetric air exchange rate in wind tunnel.

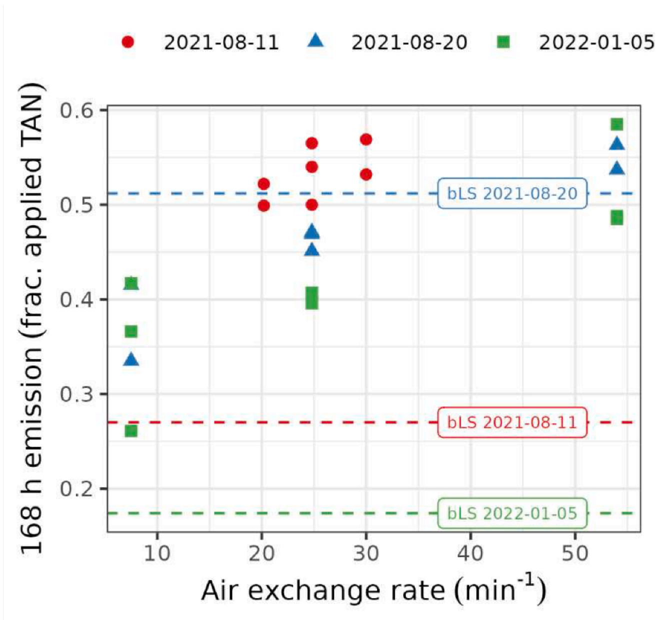

Fig. 4. Cumulative ammonia emission measured with wind tunnels (points) and bLS (dashed lines) vs. air exchange rate (applies to wind tunnel results only), showing the relationship between wind tunnel air exchange rate and measured emission, along with a comparison to bLS results.

weather conditions and slurry composition, as well as identical fields, there were substantial differences in emission between the first two August trials. Cumulative emission measured by bLS was nearly twice as high (+86 %) in the second trial compared to the first. Conversely, wind tunnel results were slightly lower in the second trial compared to the first. The reason for these differences between trials and measurement methods is not completely clear. Although rainfall was higher in the first trial (23 vs. 0.6 mm over 168 h), it occurred well after the highest fluxes were measured, and likely had only a small effect on emission. Instead, exposed slurry surface area probably contributed to bLS differences. Although not quantified, comparison of photos (supplementary material Fig. S2) shows obviously greater slurry spreading and a larger exposed surface area for the second trial. Similar photos were not taken for the wind tunnels, but slurry was applied manually there. This issue highlights the potential importance of variables such as exposed slurry surface area, that are not commonly measured or difficult to assess when measuring ammonia loss after slurry application.

Wind tunnel air exchange rate (AER) had a clear effect on measured emission, with a similar response in the two trials where it varied widely ($p = 1{\cdot}10^{-5}$ for AER effect, $p = 0.99$ for interaction based on an F test from a linear regression model). Both the second and third trials showed an increase in volatilization with AER through the entire AER range, with no indication of a plateau. In contrast, earlier studies with smaller dynamic chambers reported a plateau in NH_3 flux (Kissel et al., 1977; Bacon et al., 1986) or calculated mass transfer coefficient (Sommer and Ersbøll, 1996) below an AER of 20 min^{-1}. The smaller size of those chambers compared to the wind tunnels used here almost certainly contributed to these different responses. The effect of AER is, unfortunately, not equivalent among chamber designs. For example, the wind tunnel of Ryden and Lockyer (1985) was applied with measured air speed of 1.2 to 2.4 m s^{-1}, corresponding to AER of 36 to 72 min^{-1} for the 2 m length chambers. Even at these high levels, change in NH_3 flux with changing air speed was apparent.

Although both measurement methods showed a similar qualitative trajectory in emission, there were substantial differences between wind tunnel and bLS results (Figs. 3 and 4). Ammonia flux measured with the two methods was close during multiple periods within each trial (see first row of plots in Fig. 3). But differences were large enough and persisted long enough to lead to generally higher wind tunnel cumulative emission. Not surprisingly, differences in flux between the two methods appeared to be related to changes in weather. While both wind tunnel and bLS flux are expected to respond to air temperature, bLS is also expected to respond to changes in natural wind. This mechanism likely accounts for the difference soon after the start of the first trial, which approximately coincided with a steep drop in wind speed, as well as the tendency for smaller diurnal variation in wind tunnel results (Fig. 3). Although several bLS intervals were removed early on in the filtering process, it is unlikely that these contributed to the observed difference between the methods. Periods were filtered out during periods with low wind speed when emission was likely low, and interpolated values used to calculate cumulative emission (see Section 2.3.2) should provide a reasonable approximation of actual flux.

Only for the second August trial were some of the cumulative emission values measured with wind tunnels lower than the bLS result, which was much higher than the other bLS results (Fig. 4). Taken alone, these results suggest that an AER of around 40 would provide emission measurements comparable to bLS. However, this result applies only to this particular field trial (20 August 2021); results show clearly that there is no single wind tunnel AER that can replicate bLS measurements (Fig. 4). Instead, air flow would need to be adjusted between or even within trials (Sommer and Misselbrook, 2016). The two measurement methods are compared further with the aid of the ALFAM2 model below (Section 3.2).

Measured pH of the slurry surface after application showed a rapid increase of more than half a pH unit (Fig. S3). This general pattern has been observed elsewhere and is likely related to loss of CO_2 (Hafner et al., 2013; Pedersen, Andersson et al., 2021). Surface pH tended to decline several hours after application, and trajectories and differences between covered and open locations were not consistent between the trials.

3.2. ALFAM2 model application

The ALFAM2 model with the latest public default parameter set (set 2) (Table S1) approximately replicated the trajectory of bLS flux but tended to predict higher initial flux and a steeper drop in flux during the first day (Fig. 5). The model also missed later low peaks in flux that occurred in the days following application. Calculated cumulative emission (168 h) was quite close to bLS results for the first and last trials, but the model underestimated cumulative emission from the second August trial by a factor of 2, similar to the difference in bLS measurements between the two trials (Fig. 6), which was likely related to differences in slurry surface area or coverage (Section 3.1). The model underestimated wind tunnel cumulative emission for all trials using the default parameter set 2. Performance in replicating the wind tunnel measurements is not particularly meaningful, because of known problems with substituting average wind tunnel air velocity with natural or open-air wind speed (Section 2.4 in Andersson et al., 2023). But it highlights the challenges in interpreting wind tunnel measurements in terms of absolute emission as well as use of wind tunnel measurements in parameter estimation.

Experimental parameter set E, which accommodates differences between wind tunnel and bLS measurements, performed reasonably well, and substantially better than parameter set 2 for both types of measurements (Figs. 6 and S4). Changes in flux soon after application were not completely captured, but error was small over the complete trial (Fig. S4) and relative error in final cumulative emission was generally below 20 % of measured emission (Fig. 6). Any increase in flux over time that is not correlated with an increase in temperature or wind speed (air velocity) is inconsistent with the model structure, where the flux from each of two pools is proportional to the quantity of TAN remaining. Observed increases were measured by both methods in multiple plots, including over periods where wind speed and air temperature decreased. In the first and second trials, flux increased from the

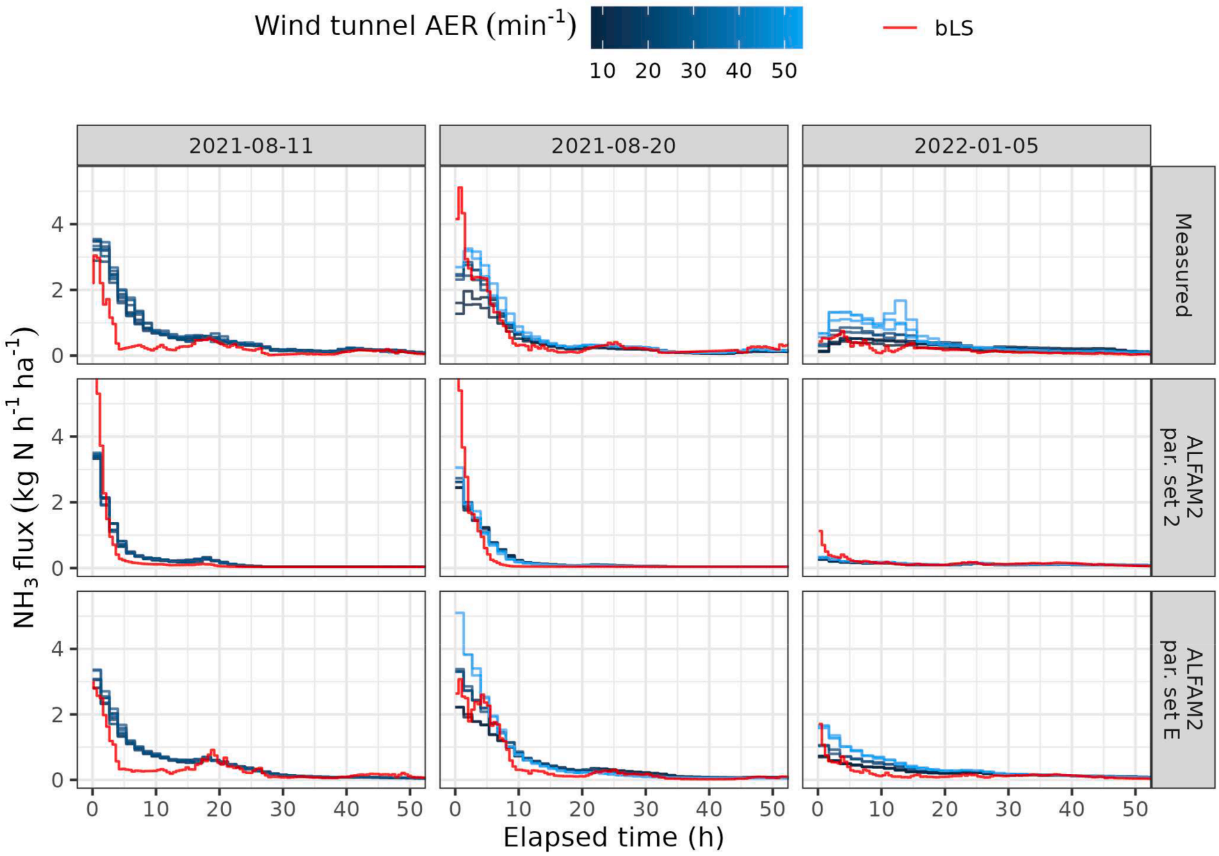

Fig. 5. Ammonia flux measured by wind tunnel or bLS (top row) or calculated using the ALFAM2 model. Experimental parameter set E (bottom row) has a single set of parameter values applied to all plots. Initial flux for the default parameter set (set 2) predictions (middle row) for the August measurements is off scale (around 10 kg h^{-1} ha^{-1}). The x axis is truncated to facilitate comparison of fluxes soon after application. For 7 d plots see Fig. S5. AER: volumetric air exchange rate in wind tunnel.

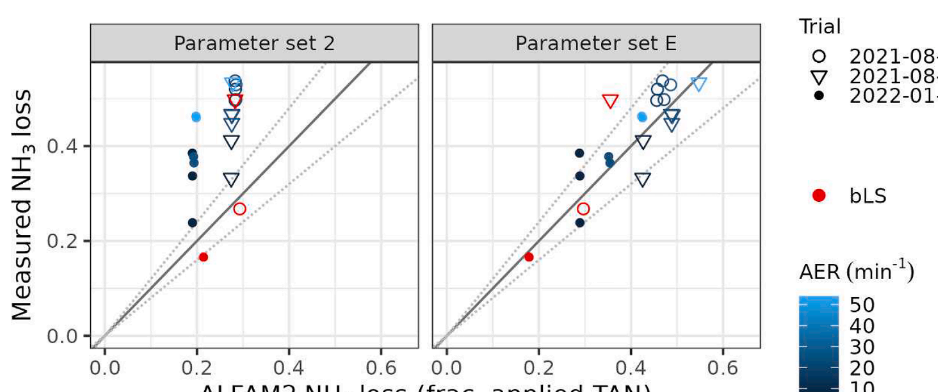

Fig. 6. Comparison between measured cumulative ammonia emission and values calculated with the ALFAM2 model using parameter set 2 and E (all as fraction of applied TAN). Values are for 168 h. Dotted lines show ± 20 %. AER: volumetric air exchange rate.

first to second measurement intervals for bLS and wind tunnel measurements (by a maximum of about 20 %) but then decreased (Fig. 3). This increase may have been due to measurement lag (instrument response lagging behind a rapid increase in NH_3 concentration), related to saturation of NH_3 adsorption on tubing or transport of NH_3 from the source to the sampling points. In the third trial, the increase occurred over the first several hours, and this explanation is less plausible. The increase in surface pH that occurred (Fig. S3) may have caused this response. In the model, slurry pH is assumed to be constant, and inclusion of this increase in a simple model would be challenging (Hafner et al., 2013). Fortunately, the contribution of this apparent error is relatively small (Fig. S4). Apart from this particular challenge of observed increasing flux, the ALFAM2 model structure seems well-suited to describe NH_3 emission dynamics. Consistent with measurements, calculated values included diurnal patterns that diminished over time as TAN was depleted and transferred to the slow pool, according to the ALFAM2 conceptual model. These diurnal patterns were somewhat weaker in experimental parameter set E results than in measurements (Fig. 5). In the model, these responses are related to an increase in r_1 due to temperature (and for bLS, wind speed) increases. In reality loss from dew during evaporation could contribute as well (Wentworth et al., 2016). Early high bLS emission in the second August trial seemed inconsistent with later rates and results from the other two trials, according to the model predictions, which effectively account for the differences in weather and slurry composition (Figs. 5 and S4). As discussed above (Section 3.1) this discrepancy may be related to exposed slurry surface area, which is not typically measured and is not a predictor variable for either parameter set applied here.

Performance of the model with experimental parameter set E provides some indication of the degree to which the model structure accurately captures the underlying emission processes, and whether differences between wind tunnel and bLS measurements can be attributed only to air-side mass transfer and rainfall (Section 2.4). From this perspective, results (Figs. 5 and 6) are encouraging. Much (not all) of the difference between bLS and wind tunnel cumulative emission (Fig. 6) and flux (Fig. 5) was reproduced by the model. Differences among the three application dates were also reproduced relatively well, especially for wind tunnel measurements. Compared to parameter set 2, set E has more TAN in the fast pool (larger f_0 intercept), but a lower emission rate constant for the fast pool (r_1) (especially for wind tunnels), along with a higher sensitivity to wind speed (Table S1). Even for bLS results, the resulting predictions match measurements much better than set 2.

According to the conceptual model represented by experimental parameter set E, wind tunnel and bLS emission differ because air-side mass transfer differs, as reflected by different values of r_1 and r_3 for the two measurement methods (Section 2.4). The effect of no rainfall in wind tunnels is captured through a difference in an input variable, not a model parameter. The relatively good performance of the ALFAM2 model with parameter set E supports this conceptual model. Parameter values (Table S1) indicate that wind tunnels have a larger intercept term for both r_1 and r_3, with roughly the same quite large relative difference (0.8–0.9 for $\log_{10}$-transformed values, or about 7-fold larger for wind tunnels). All these differences between bLS and wind tunnel parameter values are large compared to standard error estimates, implying that they are meaningful (see Table S1 for values). Parameters for the response to air speed or velocity are similar for the two methods. Model parameters r_1 and r_3 lump multiple processes (or sources of mass transfer resistance) together, so results do not conclusively show that observed differences between the measurement methods are due to differences in mass transfer within air only, but they are consistent with that interpretation.

In the ALFAM2 model, the value of r_1 determines early loss of NH_3. Calculated r_1 values show overlap between the two measurement methods for some AER values within each of the three trials (Fig. S6). While bLS values of r_1 change with diurnal patterns in both air temperature and wind, only temperature affects values for these wind tunnels with constant air flow. Therefore, the range of wind tunnel mass transfer values (r_1 and r_3) will generally not be as large as those for bLS or other micrometeorological methods (unless two different functions are used to link primary parameter values to air velocity or wind speed). The stretched appearance of the r_1 curves for the highest air velocities (Fig. S6) is, within the model, due to the log-linear relationship between air velocity and r_1 that was assumed. A square root transformation of speed and velocity slightly improved the fit and was used here. There was no overlap for r_3, which defines the rate of NH_3 loss from the slow TAN pool.

In the model, and in reality, weather variables do not independently determine emission. At very cold temperatures, for example, even the highest wind speeds will not cause high fluxes. In the actual slurry-atmosphere system, this effect is caused by a reduction in the gaseous concentration of NH_3 at the slurry surface. In the model, the log-linear relationships used for calculation of primary parameters ensure a low value of r_1 at low temperature. This effect explains the low and only weakly diurnal patterns in r_1 values for the January trial (Fig. S6), which are generally reflected in measured flux as well (Fig. 2). Infiltration of TAN into the soil may have a somewhat similar effect as low temperature. In the model, this process is represented by transfer from the fast to slow pool, which explains the low flux observed after the initial decline, despite high values of r_1 later (Figs. 2 and S4). These results generally support the ALFAM2 model structure, including the way that weather variables enter the model.

3.3. Implications for emission measurement

3.3.1. Differences between micrometeorological and wind tunnel results

Measurements and results of the ALFAM2 application presented in this work are consistent with earlier work that shows that wind tunnel and micrometeorological methods for measuring NH_3 loss are not equivalent (Scotto di Perta et al., 2019; Andersson et al., 2023). Moreover, wind tunnel average air velocity is a poor surrogate for natural wind speed with the wind tunnel design used in the present work, as shown perhaps most clearly by the differences between measurement methods apparent in r_1 model parameter values, where wind tunnels have a larger intercept term and a coefficient for air velocity that is similar to the bLS wind speed term (Table S1), resulting in a tendency for higher values of r_1 in these trials (Fig. S6). This result is consistent with earlier work that showed that mass transfer will generally be greater within wind tunnels if average air velocity is matched with external wind speed (Loubet, Cellier, Gënermont, et al., 1999). The small air inlet (Section 2.3.1) likely contributes to high turbulence within these tunnels, affecting mass transfer. In other designs with broad inlets (often equal to the cross-sectional area) (Ryden and Lockyer, 1985) or features for reducing turbulence (Scotto di Perta et al., 2016) the relationship between mass transfer and air velocity almost certainly differs. Experiments where air velocity or speed within a wind tunnel is varied to match external wind suggest that this relationship can be similar within and outside these more conventional wind tunnels (Ryden and Lockyer, 1985; Mannheim et al., 1995). But the analysis presented here shows that wind tunnel and micrometeorological measurements should not be assumed to be equivalent in general.

3.3.2. Uncertainty in bLS measurements

It is generally assumed that bLS and other micrometeorological methods provide more accurate estimates of emission under natural conditions than do wind tunnels (see Introduction), but error in bLS measurements should not be discounted. The accuracy of the bLS model is influenced by sensor height and wind direction offset, with wind direction offset being the most import when measuring outside the source area (Lemes et al., 2023). The overall uncertainty of emissions measured with the bLS model is a combination of concentration measurement uncertainty, which is instrument and inlet dependent, uncertainties in the input parameters for the model, and the bLS model output CE_{bLS}, which is dependent on number of touch-downs inside the source area and the number of trajectories. Although the estimates of total emission are likely relatively accurate (notwithstanding filtering and gap filling errors), measurement error may be much higher in individual intervals (Flesch et al., 2004; McBain and Desjardins, 2005; Harper et al., 2010; Yang et al., 2016). These errors likely affect the results presented here, and effects are difficult to quantify. For all three trials, the measurement position for bLS concentration was inside the source, which eliminates the issue of ammonia deposition between the source and sensor.

3.3.3. Interpretation and use of wind tunnel results

Interpretation of wind tunnel results in terms of emission that will occur in practice (even relative effects) is strengthened when it can be shown that wind tunnel results are similar to measurements made with micrometeorological methods. The model analysis shows some overlap, although it also shows that wind tunnel emission dynamics cannot exactly match bLS results without changes in air velocity over time, consistent with other experimental studies (Ryden and Lockyer, 1985; Mannheim et al., 1995) and a literature review (Sommer and Misselbrook, 2016). Although r_1 values tend to be higher for the wind tunnels here, the overlap in values, especially for the lower AERs used in the second August trial, do suggest that these wind tunnels can provide emission measurements that could plausibly occur under natural conditions. Unfortunately, the unusually high bLS results for this trial (Section 3.1) do not support similarity between low AER and bLS results. Certainly, additional comparisons in field trials, perhaps with quantification of the area covered with slurry, would be useful.

In contrast to the values of r_1, differences in r_3 are large and consistent, with lower values for bLS (Fig. S7). Parameter values clearly reflect persistent differences in NH_3 flux in the first and last trials, where bLS measurements showed much lower flux and less diurnal variation (Fig. S8). The cause of this pattern is not obvious, but it is not certain to be related only to air-side transport processes, as proposed above (Section 2.4). Higher turbulence and likely pressure oscillations could perhaps drive dispersion through gas pores in the slurry-soil mixture at the surface, as proposed for silage in a wind tunnel (Hafner et al., 2012) and straw mulch and other high-porosity materials in natural conditions (Hanks and Woodruff, 1958). Alternatively, the observed differences in measured flux might be primarily due to the rain that fell in these two trials, which is expected to reduce bLS but not wind tunnel flux by transporting TAN downward away from the surface. Although rainfall increases the rate of TAN transfer from the fast to slow pool in the model (through the r_2 parameter), the default effect may be too small (indeed parameter set E has a larger effect), and furthermore, there is no means of changing the quantity of TAN within the slow pool in this structure (Fig. 2). Inclusion of an additional non-emitting pool would address this model shortcoming and may resolve this issue. Differences in surface drying, nighttime cooling and daytime heating, or even slurry coverage or infiltration at the time of application may have also played a role in the observed differences. Regardless, there is a clear difference between methods. But the difference does not necessarily limit the utility of this wind tunnel design in estimating differences in emission under natural conditions among e.g., application methods or slurry types, because calculated cumulative emission is dominated by losses from the fast pool, which is controlled by r_1 (along with f_0 and r_2). As with other results presented in this work, additional comparisons are needed; this r_3 difference is based on results from only two bLS plots.

The ability of the ALFAM2 model to approximately replicate emission measurements made with both methods supports the use of wind tunnel measurements along with micrometeorological results for estimation of parameter values. Of course, parameters related to wind tunnel air velocity and intercept terms for r_1 and r_3 should not be applied to natural conditions, but it is reasonable to expect that all other model parameters could be applied under these conditions to estimate "actual" emission. Differences in wind tunnel design should be considered, however. The wind tunnel-specific parameters included in set E will almost certainly vary with wind tunnel design. This presents a challenge for parameter estimation. Grouping wind tunnel measurements by design and air velocity or air exchange rate and comparing them to average micrometeorological responses may solve this challenge.

4. Conclusions

A combination of direct comparison of emission measurements and interpretation with the aid of a model confirms that wind tunnel and bLS emission measurements differ primarily because of differences in mass transfer above the emitting surface and rainfall. This result supports the common assumption that micrometeorological methods such as bLS are a better choice for estimation of absolute emission and estimation of model parameters. But similarity in mass transfer in the two methods inferred from the model application confirms that it is reasonable to use wind tunnels to quantify relative effects of application methods or other variables. Successful use of the ALFAM2 model for interpretation of differences in emission provides a template for integrating or comparing measurements from different methods, and suggests that a combination of wind tunnel and micrometeorological measurements may be useful for evaluation or estimation of emission model parameter values.

CRediT authorship contribution statement

Sasha D. Hafner: Conceptualization, Methodology, Software, Validation, Formal analysis, Data curation, Writing – original draft, Writing – review & editing, Visualization. **Jesper N. Kamp:** Conceptualization, Methodology, Validation, Formal analysis, Investigation, Data curation, Writing – review & editing. **Johanna Pedersen:** Conceptualization, Methodology, Validation, Formal analysis, Investigation, Data curation, Writing – original draft, Writing – review & editing.

Declaration of Competing Interest

The authors declare that they have no known competing financial interests or personal relationships that could have appeared to influence the work reported in this paper.

Data availability

There are links to the data in the manuscript.

Acknowledgments

The authors would like to thank the technical staff Heidi Grønbæk, Leonid Mshanetskyi, and Peter Storgård Nielsen for their skillful help with carrying out the field trials and laboratory analysis and Jens Bonderup Kjeldsen for drone pictures. The authors would like to express their gratitude to Anders Peter S. Adamsen and Sven G. Sommer for helpful review of the manuscript draft.

Funding

This work was funded by the Ministry of Food, Agriculture and Fisheries of Denmark through two green development and demonstration programs (GUDP) with the project titles *eGylle* (journal nr.: 34009–20–1751) and Methods for reducing ammonia loss and increased methane yield from biogas slurry (MAG) (journal nr.: 34009–21–1829). Additional funding was provided by the German Federal Ministry of Food and Agriculture through the *ALFAMI* project.

Supplementary materials

Supplementary material associated with this article can be found, in the online version, at doi:10.1016/j.agrformet.2023.109790.

References

Abanades, S., Abbaspour, H., Ahmadi, A., Das, B., Ehyaei, M.A., Esmaeilion, F., El Haj Assad, M., Hajilounezhad, T., Jamali, D.H., Hmida, A., Ozgoli, H.A., Safari, S., AlShabi, M., Bani-Hani, E.H., 2022. A critical review of biogas production and usage with legislations framework across the globe. Int. J. Environ. Sci. Technol. 19 (4), 3377–3400. https://doi.org/10.1007/s13762-021-03301-6.

American Public Health Association, 1999. Standard methods for the examination of water and wastewater. In: Clescerl, L.S., Greenberg, A.E., Aeaton, A.D. (Eds.), American Public Health Association, American Water Works Association, 20th ed. Water Environment Federation.

Andersson, K., Delin, S., Pedersen, J., Hafner, S.D., Nyord, T., 2023. Ammonia emissions from untreated, separated and digested cattle slurry – Effects of slurry type and application strategy on a Swedish clay soil. Biosyst. Eng. 226, 194–208. https://doi.org/10.1016/j.biosystemseng.2023.01.012.

Aneja, V.P., Schlesinger, W.H., Erisman, J.W., 2009. Effects of agriculture upon the air quality and climate: research, policy, and regulations. Environ. Sci. Technol. 43 (12), 4234–4240. https://doi.org/10.1021/es8024403.

Association of Official Analytical Chemists, 1999. In: Cunniff, P. (Ed.), Official Methods of Analysis of AOAC International, 16th ed. AOAC.

Bacon, P.E., Hoult, E.H., McGarity, J.W., 1986. Ammonia volatilization from fertilizers applied to irrigated wheat soils. Fertil. Res. 10 (1), 27–42. https://doi.org/10.1007/BF01073903.

Bell, M.J., Hinton, N.J., Cloy, J.M., Topp, C.F.E., Rees, R.M., Williams, J.R., Misselbrook, T.H., Chadwick, D.R., 2015. How do emission rates and emission factors for nitrous oxide and ammonia vary with manure type and time of application in a Scottish farmland? Geoderma 264, 81–93. https://doi.org/10.1016/j.geoderma.2015.10.007.

Bühler, M., Häni, C., Ammann, C., Mohn, J., Neftel, A., Schrade, S., Zähner, M., Zeyer, K., Brönnimann, S., Kupper, T., 2021. Assessment of the inverse dispersion method for the determination of methane emissions from a dairy housing. Agric. For. Meteorol. 307 https://doi.org/10.1016/j.agrformet.2021.108501.

Businger, J.A., 1985. Evaluation of the accuracy with which dry deposition can be measured with current micrometeorological techniques. J. Clim. Appl. Meteorol. 25 (8), 100–1124.

Byrd, R.H., Lu, P., Nocedal, J., Shu, C., 1995. A limited memory algorithm for bound constrained optimization. SIAM J. Sci. Comput. 16, 1190–1208. https://doi.org/10.1137/0916069.

Davison, A.C., Hinkley, D.V., 1997. Bootstrap Methods and Their Application, Cambridge Series in Statistical and Probabilistic Mathematics. Cambridge University Press, Cambridge. https://doi.org/10.1017/CBO9780511802843.

Eklund, B., 1992. Practical guidance for flux chamber measurements of fugitive volatile organic emission rates. J. Air Waste Manage. Assoc. 42 (12), 1583–1591. https://doi.org/10.1080/10473289.1992.10467102.

Fangueiro, D., Hjorth, M., Gioelli, F., 2015. Acidification of animal slurry - a review. J. Environ. Manag. 149, 46–56. https://doi.org/10.1016/j.jenvman.2014.10.001.

Fangueiro, D., Pereira, J.L.S., Macedo, S., Trindade, H., Vasconcelos, E., Coutinho, J., 2017. Surface application of acidified cattle slurry compared to slurry injection: impact on NH3, N2O, CO2 and CH4 emissions and crop uptake. Geoderma 306 (June), 160–166. https://doi.org/10.1016/j.geoderma.2017.07.023.

Flesch, T.K., Wilson, J.D., Harper, L.A., 2005. Deducing ground-to-air emissions from observed trace gas concentrations: a field trial with wind disturbance. J. Appl. Meteorol. 44 (4), 475–484. https://doi.org/10.1175/JAM2214.1.

Flesch, T.K., Wilson, J.D., Harper, L.A., Crenna, B.P., Sharpe, R.R., 2004. Deducing ground-to-air emissions from observed trace gas concentrations: a field trial. J. Appl. Meteorol. 43 (3), 487–502. https://doi.org/10.1175/1520-0450(2004)043<0487:DGEFOT>2.0.CO;2.

Génermont, S., Cellier, P., 1997. A mechanistic model for estimating ammonia volatilization from slurry applied to bare soil. Agric. For. Meteorol. 88, 145–167. https://doi.org/10.1016/S0168-1923(97)00044-0.

Hafner, S.D., Haeni, C., and Fuss, R. (2022). ALFAM2: model on Ammonia Emission from Field-Applied Manure. R package version 2.1.3. https://github.com/sashahafner/ALFAM2.

Hafner, S.D., Montes, F., Alan Rotz, C., 2013. The role of carbon dioxide in emission of ammonia from manure. Atmos. Environ. 66, 63–71. https://doi.org/10.1016/j.atmosenv.2012.01.026.

Hafner, S.D., Montes, F., Rotz, C.A., 2012. A mass transfer model for VOC emission from silage. Atmos. Environ. 54, 134–140. https://doi.org/10.1016/j.atmosenv.2012.03.005.

Hafner, S.D., Nyord, T., Sommer, S.G., Adamsen, A.P.S., 2021. Estimation of Danish Emission Factors For Ammonia from Field-Applied Liquid Manure For 1980 to 2019. Advisory report from DCA - National Center for Food and Agriculture, Aarhus University, Denmark, p. 143. https://pure.au.dk/portal/files/223538048/EFreport23092021.pdf.

Hafner, S.D., Pacholski, A., Bittman, S., Burchill, W., Bussink, W., Chantigny, M., Carozzi, M., Génermont, S., Häni, C., Hansen, M.N., Huijsmans, J., Hunt, D., Kupper, T., Lanigan, G., Loubet, B., Misselbrook, T., Meisinger, J.J., Neftel, A., Nyord, T., Sommer, S.G., 2018. The ALFAM2 database on ammonia emission from field-applied manure: description and illustrative analysis. Agric. For. Meteorol. 258, 66–79. https://doi.org/10.1016/j.agrformet.2017.11.027. August 2017.

Hafner, S.D., Pacholski, A., Bittman, S., Carozzi, M., Chantigny, M., Génermont, S., Häni, C., Hansen, M.N., Huijsmans, J., Kupper, T., Misselbrook, T., Neftel, A., Nyord, T., Sommer, S.G., 2019. A flexible semi-empirical model for estimating ammonia volatilization from field-applied slurry. Atmos. Environ. 199, 474–484. S1352231018308069.

Hafner, S.D., Adani, F., Bittman, S., Burchill, W., Bussink, W., Carozzi, M., Carton, O.T., Chantigny, M., Döhler, H., Génermont, S., Häni, C., Hansen, M.N., Huijsmans, J., Hunt, D., Hutchings, N., Kamp J., Nørlem J., Kupper, T., Lanigan, G., Loubet, B., … Zilio, M.. (2023). The ALFAM2 dataset on ammonia loss from field-applied manure (v2.22) [Data set]. Zenodo. https://doi.org/10.5281/zenodo.7868172.

Hafner, S.D., Pedersen, J., and Kamp, J.N.. (2023). Comparison of wind tunnel and bLS measurement of ammona volatilization from field-applied slurry (v1.1) [Data set]. Zenodo. https://doi.org/10.5281/zenodo.8406138.

Häni, C., Flechard, C., Neftel, A., Sintermann, J., Kupper, T., 2018. Accounting for field-scale dry deposition in backward Lagrangian stochastic dispersion modelling of NH3 emissions. Atmosphere 9 (4), 1–23. https://doi.org/10.3390/atmos9040146.

Hanks, R.J., Woodruff, N.P., 1958. Influence of wind on water vapor transfer through soil, gravel, and straw mulches. Soil Sci. 86 (3), 160–164. https://doi.org/10.1097/00010694-195809000-00010.

Harper, L.A., Flesch, T.K., Weaver, K.H., Wilson, J.D., 2010. The effect of biofuel production on swine farm methane and ammonia emissions. J. Environ. Qual. 39 (6), 1984–1992. https://doi.org/10.2134/jeq2010.0172.

Houlton, B.Z., Almaraz, M., Aneja, V., Austin, A.T., Bai, E., Cassman, K.G., Compton, J.E., Davidson, E.A., Erisman, J.W., Galloway, J.N., Gu, B., Yao, G., Martinelli, L.A., Scow, K., Schlesinger, W.H., Tomich, T.P., Wang, C., Zhang, X., 2019. A world of cobenefits: solving the global nitrogen challenge. Earths Future 7 (8), 865–872. https://doi.org/10.1029/2019EF001222.

Huijsmans, J.F.M., Schröder, J.J., Mosquera, J., Vermeulen, G.D., Ten Berge, H.F.M., Neeteson, J.J., 2016. Ammonia emissions from cattle slurries applied to grassland: should application techniques be reconsidered? Soil Use Manag. 32 (June), 109–116. https://doi.org/10.1111/sum.12201.

Huijsmans, J.F.M., Vermeulen, G.D., Hol, J.M.G., Goedhart, P.W., 2018. A model for estimating seasonal trends of ammonia emission from cattle manure applied to grassland in the Netherlands. Atmos. Environ. 173 (2018), 231–238. https://doi.org/10.1016/j.atmosenv.2017.10.050.

International Organization for Standardization. (1984). Water quality - Determination of ammonium - Part 1: manual spectrometric method (ISO Standard 7150-1:1984). https://www.iso.org/standard/13742.html.

Jiang, K., Bliss, P.J., Schulz, T.J., 1995. The development of a sampling system for determining odor emission rates from areal surfaces: part 1. Aerodynamic performance. J. Air Waste Manage. Assoc. 45 (10), 831–832. https://doi.org/10.1080/10473289.1995.10467424.

Kamp, J.N., Chowdhury, A., Adamsen, A.P.S., Feilberg, A., 2019. Negligible influence of livestock contaminants and sampling system on ammonia measurements with cavity ring-down spectroscopy. Atmos. Meas. Tech. 12 (5), 2837–2850. https://doi.org/10.5194/amt-12-2837-2019.

Kamp, J.N., Häni, C., Nyord, T., Feilberg, A., Sørensen, L.L., 2021. Calculation of NH3 emissions, evaluation of backward Lagrangian stochastic dispersion model and aerodynamic gradient method. Atmosphere 12 (102). https://doi.org/10.3390/atmos12010102.

Kissel, D.E., Brewer, H.L., Arkin, G.F., 1977. Design and test of a field sampler for ammonia volatilization. Soil Sci. Soc. Am. J. 41 (6), 1133–1138. https://doi.org/10.2136/sssaj1977.03615995004100060024x.

Lemes, Y.M., Häni, C., Kamp, J.N., Feilberg, A., 2023. Evaluation of open and closed path sampling systems for determination of emission rates of NH3 and CH4 with inverse dispersion modelling. Atmos. Meas. Tech. 16, 1295–1309. https://doi.org/10.5194/amt-16-1295-2023.

Loubet, B., Cellier, P., Flura, D., Génermont, S., 1999. An evaluation of the wind-tunnel technique for estimating ammonia volitization from land: part 1. Analysis and improvement of accuracy. J. Agric. Eng. Res. 72 (71), 71–81.

Loubet, B., Cellier, P., Génermont, S., Flura, D., 1999. An evaluation of the wind-tunnel technique for estimating ammonia volatilization from land: part 2. Influence of the tunnel on transfer processes. J. Agric. Eng. Res. 72 (1), 83–92. https://doi.org/10.1006/jaer.1998.0349.

Loubet, B., Génermont, S., Ferrara, R., Bedos, C., Decuq, C., Personne, E., Fanucci, O., Durand, B., Rana, G., Cellier, P., 2010. An inverse model to estimate ammonia emissions from fields. Eur. J. Soil Sci. 61 (5), 793–805. https://doi.org/10.1111/j.1365-2389.2010.01268.x.

Mannheim, T., Braschkat, J., Marschner, H., 1995. Measurement of ammonia emission after liquid manure application: II. Comparison of the wind tunnel and the IHF method under field conditions. Z. Pflanzenernähr. Bodenk. 158, 215–219.

McBain, M.C., Desjardins, R.L., 2005. The evaluation of a backward Lagrangian stochastic (bLS) model to estimate greenhouse gas emissions from agricultural sources using a synthetic tracer source. Agric. For. Meteorol. 135 (1–4), 61–72. https://doi.org/10.1016/j.agrformet.2005.10.003.

McCollough, M.R., Pedersen, J., Nyord, T., Sørensen, P., Melander, B., 2022. Ammonia emissions, exposed surface area, and crop and weed responses resulting from three post-emergence slurry application strategies in cereals. Agronomy 12, 2441. https://doi.org/10.3390/agronomy12102441.

Misselbrook, T.H., Nicholson, F.A., Chambers, B.J., Johnson, R.A., 2005. Measuring ammonia emissions from land applied manure: an intercomparison of commonly used samplers and techniques. Environ. Pollut. 135, 389–397. https://doi.org/10.1016/j.envpol.2004.11.012, 3 SPEC. ISS.

Nyord, T., Søgaard, H.T., Hansen, M.N., Jensen, L.S., 2008. Injection methods to reduce ammonia emission from volatile liquid fertilisers applied to growing crops. Biosyst. Eng. 100 (2), 235–244. https://doi.org/10.1016/j.biosystemseng.2008.01.013.

Pedersen, J., Nyord, T., Feilberg, A., Labouriau, R., 2021. Analysis of the effect of air temperature on ammonia emission from band application of slurry. Environ. Pollut. 282, 117055. https://doi.org/10.1016/j.envpol.2021.117055.

Pedersen, J., Andersson, K., Feilberg, A., Delin, S., Hafner, S.D., Nyord, T., 2021. Effect of exposed surface area on ammonia emissions from untreated, separated, and digested cattle manure. Biosyst. Eng. 202, 66–78. https://doi.org/10.1016/j.biosystemseng.2020.12.005.

Pedersen, J., Feilberg, A., Kamp, J.N., Hafner, S., Nyord, T., 2020. Ammonia emission measurement with an online wind tunnel system for evaluation of manure application techniques. Atmos. Environ. 230 https://doi.org/10.1016/j.atmosenv.2020.117562. December 2019.

Pedersen, J., Hafner, S., Adamsen, A.P.S., 2022. Effectiveness of mechanical separation for reducing ammonia loss from field-applied slurry: assessment through literature review and model calculations. J. Envrion. Manag. 323 (116196) https://doi.org/10.1016/j.jenvman.2022.116196.

R Core Team, 2022. R: A Language and Environment For Statistical Computing. R foundation for statistical computing, Vienna. http://www.r-project.org.

Ryden, J.C., Lockyer, D.R., 1985. Evaluation of a system of wind tunnels for field studies of ammonia loss from grassland through volatilisation. J. Sci. Food Agric. 36 (9), 781–788. https://doi.org/10.1002/jsfa.2740360904.

Saha, C.K., Wu, W., Zhang, G., Bjerg, B., 2011. Assessing effect of wind tunnel sizes on air velocity and concentration boundary layers and on ammonia emission estimation using computational fluid dynamics (CFD). Comput. Electron. Agric. 78 (1), 49–60. https://doi.org/10.1016/j.compag.2011.05.011.

Scotto di Perta, E.S., Agizza, M.A., Sorrentino, G., Boccia, L., Pindozzi, S., 2016. Study of aerodynamic performances of different wind tunnel configurations and air inlet velocities, using computational fluid dynamics (CFD). Comput. Electron. Agric. 125, 137–148. https://doi.org/10.1016/j.compag.2016.05.007.

Scotto di Perta, E.S., Fiorentino, N., Carozzi, M., Cervelli, E., Pindozzi, S., 2020. A review of chamber and micrometeorological methods to quantify NH3 emissions from fertilisers field application. Int. J. Agron. 2020 https://doi.org/10.1155/2020/8909784.

Scotto di Perta, E.S., Fiorentino, N., Gioia, L., Cervelli, E., Faugno, S., Pindozzi, S., 2019. Prolonged sampling time increases correlation between wind tunnel and integrated horizontal flux method. Agric. For. Meteorol. 265, 48–55. https://doi.org/10.1016/j.agrformet.2018.11.005. November 2018.

Shah, S.B., Westerman, P.W., Arogo, J., 2006. Measuring ammonia concentrations and emissions from agricultural land and liquid surfaces: a review. J. Air Waste Manag. Assoc. 56 (7), 945–960. https://doi.org/10.1080/10473289.2006.10464512.

Simmons, G.F., 1996. Calculus With Analytic Geometry. McGraw-Hill Education.

Smith, R.J., Watts, P.J., 1994. Determination of odour emission rates from cattle feedlots: part 2, evaluation of two wind tunnels of different size. J. Agric. Eng. Res. 58 (4), 231–240. https://doi.org/10.1006/jaer.1994.1053.

Sommer, S.G., Ersbøll, A.K., 1996. Effect of air flow rate, lime amendments, and chemical soil properties on the volatilization of ammonia from fertilizers applied to sandy soils. Biol. Fertil. Soils 21 (1–2), 53–60. https://doi.org/10.1007/BF00335993.

Sommer, S.G., Génermont, S., Cellier, P., Hutchings, N.J., Olesen, J.E., Morvan, T., 2003. Processes controlling ammonia emission from livestock slurry in the field. Eur. J. Agron. 19, 465–486. https://doi.org/10.1016/S1161-0301(03)00037-6.

Sommer, S.G., Jensen, L.S., Clausen, S.B., Søgaard, H.T., 2006. Ammonia volatilization from surface-applied livestock slurry as affected by slurry composition and slurry infiltration depth. J. Agric. Sci. 229–235. https://doi.org/10.1017/S0021859606006022. April 2006.

Sommer, S.G., Misselbrook, T.H., 2016. A review of ammonia emission measured using wind tunnels compared with micrometeorological techniques. Soil Use Manag. 32 (June), 101–108. https://doi.org/10.1111/sum.12209.

Sommer, S.G., Olesen, J.E., Christensen, B.T., 1991. Effects of temperature, wind speed and air humidity on ammonia volatilization from surface applied cattle slurry. J. Agric. Sci. 117, 91–100.

Uwizeye, A., de Boer, I.J.M., Opio, C.I., Schulte, R.P.O., Falcucci, A., Tempio, G., Teillard, F., Casu, F., Rulli, M., Galloway, J.N., Leip, A., Erisman, J.W., Robinson, T.P., Steinfeld, H., Gerber, P.J., 2020. Nitrogen emissions along global livestock supply chains. Nat Food 1 (7), 437–446. https://doi.org/10.1038/s43016-020-0113-y.

Webb, J., Pain, B., Bittman, S., Morgan, J., 2010. The impacts of manure application methods on emissions of ammonia, nitrous oxide and on crop response-A review. Agric. Ecosyst. Environ. 137 (1–2), 39–46. https://doi.org/10.1016/j.agee.2010.01.001.

Wentworth, G.R., Murphy, J.G., Benedict, K.B., Bangs, E.J., Collett, J.L., 2016. The role of dew as a night-time reservoir and morning source for atmospheric ammonia. Atmos. Chem. Phys. 16 (11), 7435–7449. https://doi.org/10.5194/acp-16-7435-2016.

Wulf, S., Maeting, M., Clemens, J., 2002. Application technique and slurry co-fermentation effects on ammonia, nitrous oxide, and methane emissions after spreading. J. Environ. Qual. 31 (6), 1789. https://doi.org/10.2134/jeq2002.1795.

Yang, W., Zhu, A., Zhang, J., Zhang, X., Che, W., 2016. Agricultural and Forest Meteorology Assessing the backward Lagrangian stochastic model for determining ammonia emissions using a synthetic source. Agric. For. Meteorol. 216, 13–19.